Kinetic Model for the Inhibition of Actin Polymerization by Actobindin

Michael R. Bubb‡ and Edward D. Korn*

Laboratory of Cell Biology, National Heart, Lung, and Blood Institute, National Institutes of Health, Bethesda, Maryland 20892

Received November 15, 1994; Revised Manuscript Received January 23, 1995⊗

ABSTRACT: Although *Acanthamoeba* actobindin binds actin monomers, its inhibition of actin polymerization differs from that of a simple monomer-sequestering protein in that actobindin inhibits nucleation very much more than elongation [Lambooy, P. K., & Korn, E. D. (1988) *J. Biol. Chem. 263*, 12836−12843] and can induce the accumulation of actin dimers in stoichiometric excess of the actobindin concentration [Bubb, M. R., Knutson, J. R., Porter, D. K., & Korn, E. D. (1994) *J. Biol. Chem. 269*, 25592−25597]. We now describe a "catalytic" model for the interaction of actobindin with actin monomer that quantitatively accounts for the effects of actobindin on the kinetics of actin polymerization *de novo* and the elongation of actin filaments. We propose that, in a polymerizing buffer, actobindin binds to two actin subunits forming an heterotrimeric complex that is incompetent for nucleation, self-association, and elongation. Actobindin can, however, dissociate from this complex, leaving a novel actin dimer that can participate in elongation but remains incompetent for nucleation and self-association. Under appropriate conditions, the concentration of this novel actin dimer can exceed the actobindin concentration; thus, the model is catalytic rather than stoichiometric. The experimentally observed time course of actin polymerization *de novo*, the rate of elongation of filaments, and the amount of actin dimer formed as a function of actobindin concentration are all consistent with the catalytic model and inconsistent with the stoichiometric model. The rate of actobindin-induced actin dimer formation is consistent with the hypothesis that the rate-limiting step is this pathway is the formation of a precursor heterotrimeric complex.

Actobindin is a 9800-Da protein (88 amino acids) with an internal repeat of 33 amino acids (Vandekerckhove et al., 1990) isolated from *Acanthamoeba castellanii* (Lambooy & Korn, 1986). It is a potent inhibitor of actin polymerization *de novo* (i.e., nucleation plus elongation) but a much less effective inhibitor of filament elongation (Lambooy & Korn, 1988). Actobindin has two actin-binding sites (Vancompernolle et al., 1991), one in each internal repeat, that can bind actin monomers simultaneously (Bubb et al., 1991) and also, and with much higher affinity, bind cross-linked actin dimers (Bubb et al., 1994a). In addition, under polymerizing conditions, actobindin causes the formation, in excess of the actobindin concentration, of a novel actin dimer (Bubb et al., 1994b) that can neither self-associate nor nucleate polymerization but can add to the ends of actin filaments. In this paper, we propose a kinetic model that quantitatively fits the experimental data for the time course and extent of actin polymerization in the presence of actobindin as well as the rate of formation and steady-state concentration of actobindin-induced actin dimers.

MATERIALS AND METHODS

Proteins. Actobindin was purified by previously described methods (Bubb & Korn, 1991). Rabbit muscle actin was purified according to the method of Spudich and Watt (1971) and then gel-filtered over a Sephacryl HR-300 column in a buffer containing 5 mM Tris, 0.2 mM ATP, 0.2 mM dithiothreitol, 0.1 mM $CaCl_2$, and 0.01% NaN_3, pH 7.8 (buffer G). Pyrenyl-labeled actin[1] was prepared using the method of Kouyama and Mihashi (1981) and was then gel-filtered. The extent of labeling varied from 0.93 to 1.01 mol/mol. Actobindin concentration was determined by amino acid analysis and actin concentration by its absorbance at 290 nm using $E = 2.59 \times 10^4$ M^{-1} cm^{-1}.

Time Course of Actin Polymerization. Pyrenyl-labeled Ca^{2+}-G-actin (with or without actobindin) was converted to Mg^{2+}-G-actin by the addition of 50 μM $MgCl_2$ and 125 μM EGTA. The sample temperature was maintained at 18 °C. Polymerization was initiated 15 min later by the addition of $MgCl_2$ to a final concentration of 2 mM. The increase in time-averaged fluorescence emission intensity (excitation wavelength, 366 nm; emission wavelength, 386 nm) was followed in a Spex Fluorolog 212 spectrofluorometer modified by the addition of a timed shutter to prevent photobleaching. Steady-state fluorescence intensity was measured after 24−36 h. Analysis of the experimental data is described in the Results section.

Elongation Rates. Stopped-flow fluorescence data were obtained using a Bio-Logic SFM-3 stopped-flow module integrated with an SLM-Aminco 8100 spectrofluorometer with a 31-μL cuvette thermostated at 18 °C. The excitation wavelength was 366 nm with emission detected at a 90° angle from the incident beam by a photomultiplier tube. The emission signal was attenuated by a 400-nm cutoff filter. The filter was angled at approximately 5° from perpendicular to the light path to extend the transmission spectrum.

Phalloidin-stabilized seeds were prepared from unlabeled actin as suggested by Estes et al. (1981). Three syringes were used to inject (i) 250 μL of a solution containing 4.4 μM pyrenyl-labeled Mg^{2+}-G-actin (prepared as described

* To whom correspondence should be addressed at Building 3, Room B1-22, National Institutes of Health, Bethesda, MD 20892.

‡ Present address: J. Hillis Miller Health Center, University of Florida College of Medicine, Gainesville, FL 32610-0277.

⊗ Abstract published in *Advance ACS Abstracts,* March 15, 1995.

[1] Abbreviation: pyrenyl-labeled actin, (*N*-pyrenylcarboxamidoethyl)-actin.

above) and varying concentrations of actobindin, (ii) 250 μL of buffer F (buffer G plus 4.0 mM $MgCl_2$ and 125 μM EGTA), and (iii) 0−38 μL of phalloidin-stabilized F-actin seeds at an actin subunit concentration of 2.0 μM; final concentrations were approximately 2.2 μM actin, 2.0 mM $MgCl_2$, and actobindin as indicated. These concentrations are uncorrected for the small differences in volume (<8%) due to the different amounts of seed solution added. The actin and $MgCl_2$ concentrations, however, were identical for all samples containing the same concentration of seeds. Samples were injected over a time period of 400 ms. The data were analyzed using the equilibrium constants determined from the polymerization time course experiments (see Results).

Amount and Rate of Formation of Actin Dimer. To quantify the amount of actin dimer formed, 950-μL samples containing 2.2 μM pyrenyl-labeled Mg^{2+}-G-actin and 0−10 μM actobindin (prepared as described for the polymerization time course experiments) were mixed in a quartz cuvette with a long pipet tip. Baseline fluorescence intensity was determined at 18 °C, as described above, and dimer formation was then induced by addition of $MgCl_2$ to a final concentration of 2.0 mM and mixing for 15 s. The time-averaged fluorescence intensity was determined over the next 60 s, i.e., before any polymerization could occur. In several samples, the order of addition of $MgCl_2$ and actobindin was reversed, and the baseline fluorescence intensity was determined before the addition of actobindin; the fluorescence increased only after the actobindin was added.

The rate of dimer formation, as reflected by the increase in fluorescence intensity, was determined in the stopped-flow fluorescence device, as described above, using a 9-μL cuvette and a 200-ms injection time to reduce the dead time to 7.2 ms. One syringe injected 125 μL of 4.4 μM pyrenyl-labeled Mg^{2+}-G-actin containing varying concentrations of actobindin while a second syringe injected 125 μL of buffer F. Data were analyzed by the same methods used to determine the elongation rates (see Results).

THEORY

The Catalytic Model. The time course of polymerization of actin alone was modeled as summarized by Tobacman and Korn (1983). In brief, this method explicitly assumes (i) that all oligomers larger than trimer grow by sequential addition of monomers until the concentration of monomers falls to its steady-state value, the critical concentration, (ii) that the trimer is in rapid preequilibrium with monomer with an overall equilibrium constant K_n, (iii) that the elongation rate constant k_c^+ is the same for the trimer and all larger oligomers, and (iv) that the dissociation rate constant k_c^- is the same for the tetramer and all larger oligomers. Implicitly, this method assumes that actin monomer accounts for essentially all of the unpolymerized actin. With these assumptions, the rates of nucleation, $d[C_n]/dt$, and elongation, $d[A_f]/dt$, are defined by two differential equations:

$$d[C_n]/dt = K_n k_c^+ [A]^3([A] - A_o) \quad (1)$$

$$d[A_f]/dt = k_c^+[C_n][A] - k_c^-[C_n] = k_c^+[C_n]([A] - A_o) \quad (2)$$

where $[C_n]$ is the molar concentration of nuclei; $[A_f]$ is the concentration of polymerized actin subunits; [A] is the actin monomer concentration; k_c^+ and k_c^- are the sums of the rate constants for elongation and dissociation, respectively, at the two filament ends; and $A_o = k_c^-/k_c^+$ is the critical concentration of actin. Numerical integration of eqs 1 and 2 produces a curve for the time course of polymerization that is dependent on the actin concentration, the critical concentration, and a parameter $K_n(k_c^+)^2$, which is the product of the elongation rate constant k_c^+ and an apparent nucleation rate cnstant $K_n k_c^+$.

The catalytic model[2] includes the following additional interactions when actobindin is present: (i) binding of actin monomer, A, to one of either of the two actin binding sites on actobindin, B, to form AB with an association equilibrium constant, $K_1 = k_1^+/k_1^-$; (ii) the association of a second actin monomer to form A_2B with an association equilibrium constant, $K_2 = k_2^+/k_2^-$; and (iii) the loss of actobindin to form A_2' with an association equilibrium constant, $K_3 = k_3^+/k_3^-$, according to the reaction pathway:

$$2A + B \overset{1}{\rightleftharpoons} AB + A \overset{2}{\rightleftharpoons} A_2B \overset{3}{\rightleftharpoons} A_2' + B \quad (3)$$

A_2' differs from the normal intermediate in actin polymerization, A_2, in that A_2' can neither self-associate nor be a substrate for elongation, but it can add to the ends of existing filaments. In the catalytic model, neither AB nor A_2B can participate in any aspect of polymerization. As discussed below, an alternate pathway to A_2B, in which two actin monomers interact to form A_2 which then reacts with B, was also considered. The two pathways are kinetically identical and experimentally indistinguishable in terms of the products A_2B and A_2'.

The additional reactions of the catalytic model require the addition of differential eqs 4−6 to describe the kinetics of reaction pathway 3 and the modification of eq 2 to include a term, $2\beta[A_2']$, for the participation of A_2' in the elongation reaction; see eq 8. β is the ratio of the elongation rate constant for the addition of the actin dimer, A_2', to the elongation rate constant for the addition of actin monomer, k_c^+, to the two ends of growing filaments. Equation 1 remains unchanged (eq 7) because A_2' cannot participate in the nucleation reaction.

$$d[AB]/dt = k_1^+[A][B] + k_2^-[A_2B] - k_1^-[AB] - k_2^+[AB][A] \quad (4)$$

$$d[A_2B]/dt = k_2^+[AB][A] + k_3^+[A_2'][B] - k_3^-[A_2B] - k_2^-[A_2B] \quad (5)$$

$$d[A_2']/dt = k_3^-[A_2B] - k_3^+[A_2'][B] - k_c^+\beta[C_n][A_2'] \quad (6)$$

$$d[C_n]/dt = K_n k_c^+ [A]^3([A] - A_o) \quad (7)$$

$$d[A_f]/dt = k_c^+[C_n]([A] + 2\beta[A_2'] - A_o) \quad (8)$$

This treatment follows the model of Tobacman et al. (1983)

[2] We refer to this as a catalytic model because the novel dimer formed in the presence of actobindin can exceed the actobindin concentration and the dimer is either not present or undetectable in the absence of actobindin. The experimental data cannot be fit by a stoichiometric model in which actobindin simply sequesters actin dimers or two actin monomers.

for actin polymerization in the presence of the monomer binding protein, profilin, but is modified to include (i) the change from an explicit solution for [A] to an iterative solution; (ii) the introduction of terms to account for the two additional species, A_2B and A_2'; and (iii) the addition of a term in the elongation rate equation for addition of A_2'.

The time course of polymerization of actin in the presence of actobindin was determined by the iterative solution of differential eqs 4−8. The constants k_n, k_c^+, and A_o were determined from the polymerization data for actin alone, as were the constants relating fluorescence intensity to the quantity of G- and F-actin. If, however, the interaction of actobindin and actin were rapid relative to the rate of polymerization, i.e., if each of the species in eq 3 were at equilibrium at all times, the experimental data would provide information only for determination of the equilibrium constants. Thus, the best fit to these equations would be indeterminate unless one rate constant were fixed for each reaction. If this were done, and as long as the rate constants were fast enough to achieve preequilibrium, any changes in the forward and reverse rate constants for any of the reactions that did not change the equilibrium constant for that reaction would give the same predicted time course for polymerization. This condition was met computationally by selecting fixed values for the forward rate constants and documenting that the values calculated for the equilibrium constants did not vary with changes in the selected fixed values. Thus, even though the differential equations explicitly include all rate constants, the fitting algorithm [based on the Marquardt−Levenberg method (Knott, 1979)] fitted only the three parameters K_3, the product K_2K_1, and the relative elongation rate β. As K_1 is known from previous results (Bubb et al., 1991), K_2 could be calculated from the value for K_2K_1.

The Stoichiometric Model. Attempts to fit the data by the stoichiometric model used the same differential equations as developed for the catalytic model but with K_3 equal to zero because, in the stoichiometric model, A_2B does not decompose to A_2' and B.

RESULTS

Time Course of Polymerization. The model of Tobacman and Korn (1983) provided a good fit to the time course of polymerization of actin alone in 2 mM $MgCl_2$ at 18 °C (Figure 1A) with a critical concentration, A_o, of 0.30 μM and a value for $K_n(k_c^+)^2$ of 6×10^{15} s^{-2} M^{-4}. These values are very similar to those obtained 10 years earlier by Tobacman and Korn (1983), who found $A_o = 0.25$ μM and $K_n(k_c^+)^2 = 3.3 \times 10^{15}$ s^{-2} M^{-4} in 2 mM $MgCl_2$ at 25 °C.

Addition of even small amounts of actobindin significantly inhibited actin polymerization (Figure 1B). As expected if, as discussed in the previous section, actobindin and actin were in preequilibrium during polymerization, simultaneous fitting of the polymerization data for three different concentrations of actobindin gave indeterminate results for the rate constants. The data could be fit, however, as described in the Theory section, by values for K_3, K_2K_1, and β. The best fit to the experimental data (Figure 1B) was obtained with the values for K_3, K_2, K_1, and β listed in Table 1.

The polymerization time course for any single condition could also be fit by the stoichiometric model, as shown in Figure 1B for polymerization in the presence of 1.0 μM actobindin. However, the stoichiometric model was unable to fit the data for three different actobindin concentrations simultaneously (Figure 1B, dashed lines). That the catalytic model fits the experimental data better than the stoichiometric

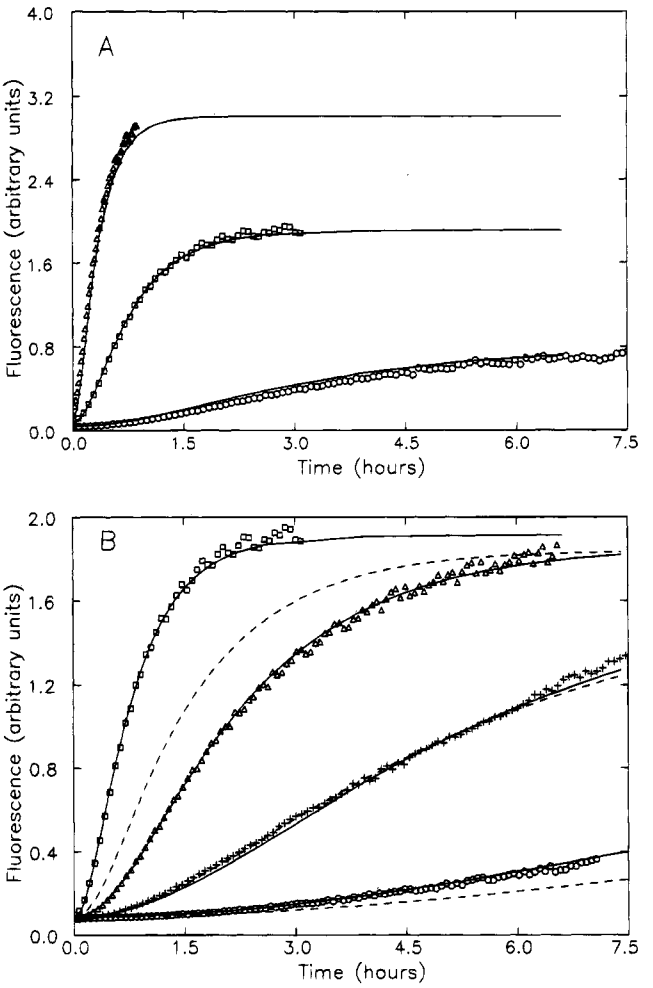

FIGURE 1: Time course of polymerization of pyrenyl-labeled Mg^{2+}-actin with and without actobindin. (Panel A) Various concentrations of actin were polymerized to steady state in the absence of actobindin: △, 3.3 μM actin; □, 2.2 μM actin; ○, 1.1 μM actin. The solid lines show the best simultaneous fit to the data with $K_n(k_c^+)^2 = 6.0 \times 10^{15}$ s^{-2} M^{-4} (see text). (Panel B) A fixed concentration of actin, 2.2 μM, was polymerized in the presence of various concentrations of actobindin: □, no actobindin; △, 0.3 μM actobindin; +, 1.0 μM actobindin; ○, 2.2 μM actobindin. The solid lines show the best simultaneous fit to the data assuming a "catalytic" model of inhibition with $K_2 = 4.4 \times 10^6$ μM^{-1}, $K_3 = 1.3 \times 10^7$ M^{-1}, and $\beta = 1.0$. The solid line for 2.2 mM actin and no actobindin is identical to that in panel A. The dashed lines show the best simultaneous fit for a "stoichiometric" model with $K_2 = 3.8 \times 10^6$ μM^{-1}.

Table 1: Kinetic Parameters for the Inhibition of Actin Polymerization by Actobindin

parameter	value[a]	source
K_1	3×10^5 M^{-1}	Bubb et al. (1991)
K_2	4.4×10^6 [$(4.1-4.6) \times 10^6$] M^{-1}	Figure 1B
α^b	59	$4K_2/K_1$
K_3	1.3×10^7 [$(1.1-1.3) \times 10^7$] M^{-1}	Figure 1B
β	0.9 (0.5−2.2)	Figure 2
k_2^+	9.0×10^6 [$(7.9-10.1) \times 10^6$] s^{-1} M^{-1}	Figure 3B

[a] The 95% confidence intervals are shown in parentheses. [b] α is a measure of cooperativity; K_2/K_1 is arbitrarily multiplied by 4 so that $\alpha = 1$ in a noncooperative, independent reaction pathway. Values greater than 1 indicate positive cooperativity, and values less than 1 may indicate negative cooperativity.

Table 2: Effect of Actobindin on the Steady-State Concentration of F-Actin: Experimental vs Predicted[a]

actobindin concn (μM)	F-actin		
	exptl (μM)	stoichiometric model (μM)	catalytic model (μM)
0.3	1.90 ± 0.04[b]	1.82	1.85
1.0	1.81 ± 0.04	1.65	1.77
2.2	1.63 ± 0.04	1.32	1.68

[a] The steady-state concentrations of F-actin determined in three experiments such as the one described in Figure 1A are compared to the values predicted by the stoichiometric and catalytic models (see text). [b] One standard deviation.

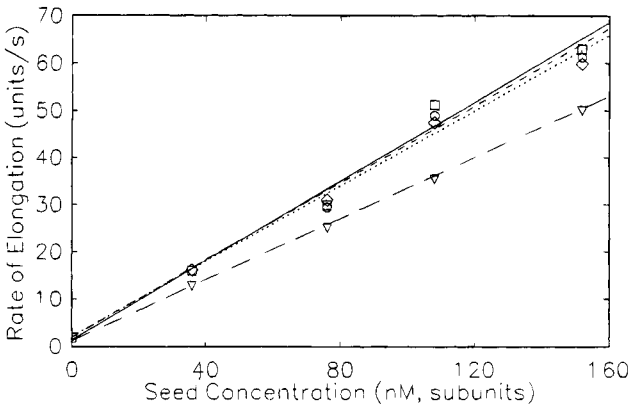

FIGURE 2: Elongation rates of F-actin in a seeded polymerization assay. Varying concentrations of phalloidin-stabilized F-actin seeds were added in a stopped-flow fluorescence apparatus to pyrenyl-labeled Mg^{2+}-G-actin (final concentration 2.2 μM), and the rate of elongation was estimated by the rate of change of fluorescence. Each data point represents the average of three or four assays. The slopes of the lines (determined by linear regression) give the relative elongation rates for various concentrations of actobindin: □ and solid line, no actobindin; ○ and dashed line, 0.7 μM actobindin; ◇ and dotted line, 1.2 μM actobindin; ▽ and long dashes, 2.2 μM actobindin. Data for 0.3 μM actobindin are not shown but were indistinguishable from the control without actobindin.

model is more apparent when the experimentally determined concentrations of F-actin at steady state are compared to the concentrations of F-actin predicted by the two models (Table 2).

Elongation Rates. Increasing concentrations of actobindin had little effect on elongation rates until the actobindin concentration was nearly equimolar with actin (Figure 2). Qualitatively, if A_2B were the only actin dimer species present, and if it did not add to F-actin (the stoichiometric model), equal increments in actobindin concentration would cause the largest increases in [A_2B] (and, therefore, the greatest decreases in the elongation rate) when the total actobindin combination was low. On the other hand, according to the catalytic model the ratio of A_2' to A_2B would be greatest at low actobindin concentration, and actobindin would be proportionately more inhibitory at high concentrations where A_2B would predominate.

The experimentally determined effect of actobindin on the elongation rate is compared to the results predicted by the catalytic and stoichiometric models in Table 3. The theoretical values were determined by (i) calculating the equilibrium concentrations of species A and A_2' from the total concentrations of actin and actobindin and the equilibrium constants in Table 1, (ii) substituting these values into eq 8 to calculate the theoretical initial polymerization rates, and (iii) comparing

Table 3: Effect of Actobindin on the Elongation Rate: Experimental vs Predicted[a]

actobindin concn (μM)	elongation rate (% of control)		
	exptl	stoichiometric model	catalytic model
0.3	100 (93−101)[b]	80	109
0.7	97 (91−103)	60	94
1.2	95 (89−101)	44	83
2.2	77 (73−81)	30	74

[a] The relative elongation rates calculated from the experiment described in Figure 2 are compared to the values predicted by the stoichiometric and catalytic models (see text). [b] 95% confidence interval.

these rates to the initial rate of polymerization of actin in the absence of actobindin, eq 2, expressed as percent of control. The experimental results are clearly in much better agreement with the catalytic model (and the assumption that A_2', but not A_2B or AB, can participate in elongation) than with the stoichiometric model.

Actobindin-Induced Actin Dimer Formation. An immediate increase in fluorescence intensity of ~12% occurred when 2.0 mM $MgCl_2$ was added to a mixture of pyrenyl-labeled Mg^{2+}-G-actin and saturating amounts of actobindin or when actobindin was added to pyrenyl-labeled Mg^{2+}-actin immediately after 2.0 mM $MgCl_2$ was added and before polymerization had started (data not shown). Neither the addition of 2 mM $MgCl_2$ to pyrenyl-labeled Mg^{2+}-G-actin, in the absence of actobindin, nor the formation of a 1:1 complex between pyrenyl-labeled Mg^{2+}-G-actin and actobindin, in the absence of 2 mM $MgCl_2$, had any effect on fluorescence under these conditions [the 1:1 complex did show a 21% increase when the excitation wavelength was 343 nm instead of the 366 nm used in these experiments (Bubb et al., 1991)]. Therefore, the observed increase in fluorescence was almost certainly due to actobindin-induced actin−actin interactions. Qualitatively similar increases in fluorescence occurred when 100 mM KCl was substituted for 2 mM $MgCl_2$, demonstrating that the fluorescence change was not related to an exchange of Mg^{2+} for any residual actin-bound Ca^{2+}. Detailed quantitative analysis, however, was carried out only for the experiments in 2 mM $MgCl_2$ to facilitate comparison to previous experiments (Bubb et al., 1994a,b) and because earlier studies had shown no difference in the effects of actobindin on actin polymerization in the presence or absence of KCl (Lambooy & Korn, 1986).

Actobindin concentrations as low as 20 nM increased the fluorescence of 2.2 μM pyrenyl-labeled Mg^{2+}-G-actin after the addition of 2.0 mM $MgCl_2$ (Figure 3A). The fluorescence continued to increase with increasing concentrations of actobindin until a plateau was reached at an actobindin concentration of about 2.0 μM. The slope of this curve was significantly greater than predicted by the stoichiometric model but could be fit quite well by the catalytic model (Figure 3A, line) using the equilibrium constants in Table 1 derived from the experiment shown in Figure 1. Similar results were obtained when the order of addition of actobindin and $MgCl_2$ was reversed (Figure 3A). The time course of fluorescence change shows that dimer formation reached steady state in less than 1 s (Figure 3B). These experimental data were accurately fit (Figure 3B) with the assumption that the increase in fluorescence was due to the formation of both A_2' and A_2B and that the rate-limiting

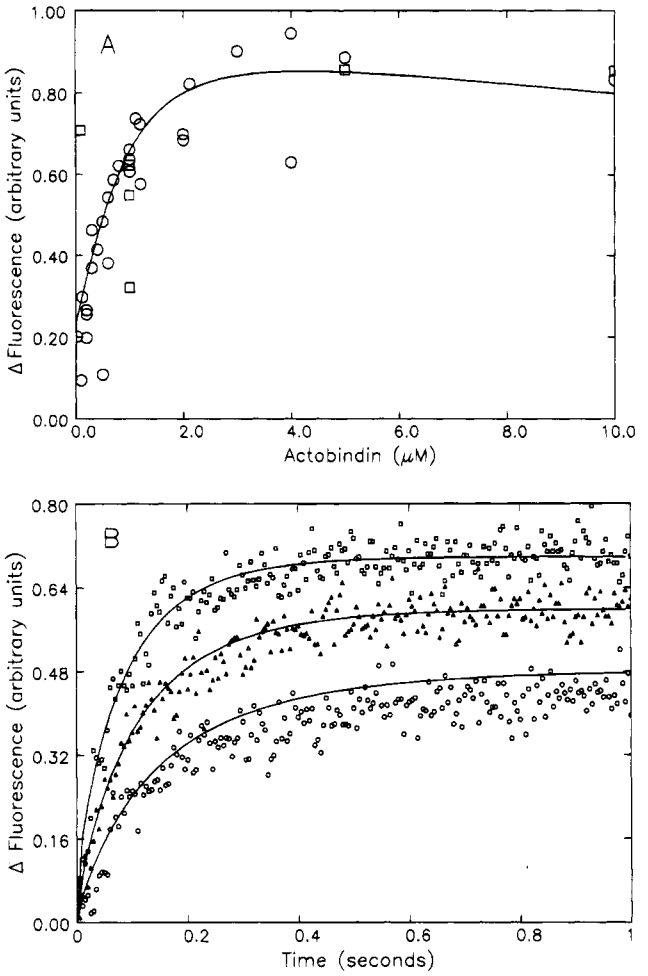

FIGURE 3: Quantity and rate of dimer formation as a function of actobindin concentration. The change in fluorescence intensity was measured after the addition of $MgCl_2$ and actobindin but before any significant polymerization had occurred. (Panel A) The steady-state increment in fluorescence after addition of $MgCl_2$ (final concentration 2.0 mM) to a mixture of actobindin and 2.2 μM pyrenyl-labeled Mg^{2+}-G-actin (□) or after addition of actobindin immediately after addition of $MgCl_2$ to actin (○). The line shows the result predicted by the catalytic model if this assay reflects the amounts of A_2B and A_2' expected from the equilibrium parameters derived from Figure 1. (Panel B) Time course of fluorescence change after addition of 2 mM $MgCl_2$ (final concentration) to 2.2 μM pyrenyl-labeled Mg^{2+}-G-actin in the presence of varying concentrations of actobindin measured by stopped-flow fluorescence: ○, 0.6 μM actobindin; △, 1.2 μM actobindin; □, 3.2 μM actobindin. The lines show the predicted result with the same assumptions as in panel A and the assumption that the formation of A_2B is rate limiting with $k_2^+ = 9.0 \times 10^6$ s^{-1}.

step was the conversion of AB to A_2B with the value of k_2^+ shown in Table 1.

DISCUSSION

The catalytic model provides a quantitative explanation for our previous observations that actobindin is a much more potent inhibitor of actin polymerization *de novo* than it is of either filament elongation or the concentration of F-actin at steady state. The catalytic model also explains the accumulation, under certain conditions, of actin dimers in molar excess of the actobindin concentration. The experimental data cannot be fit by the stoichiometric model. The catalytic model is incomplete, however, in that it does not distinguish between two alternative pathways to the ternary complex A_2B: (i) the stepwise addition of two actin monomers to actobindin and (ii) the addition of actobindin to an actin dimer species, A_2, that, in the absence of actobindin, would be a normal precursor to F-actin. In either case, A_2', the novel dimeric species formed from A_2B, is different than A_2 because A_2' does not self-associate nor nucleate polymerization. The two pathways are experimentally indistinguishable because the concentration of both postulated intermediates must be very low: A_2 because actin polymerization can be successfully modeled (Figure 1A) by the equations of Tobacman and Korn (1983) which assume that all intermediates between monomeric actin and F-actin are at very low concentrations and AB because K_1 is small relative to K_2 (Table 1).

Although the experimental data do support a truly catalytic role for actobindin (best seen in Figure 3A at very low actobindin concentrations), not all of the data are in strict accord with the catalytic model in its simplest form. According to the model, under the conditions described in Figure 3A trace amounts of actobindin should convert more than one-fifth of the total actin to A_2'. This should result in more rapid elongation than in the absence of actobindin because the elongation rate constants for addition of A_2' and A to filaments are almost identical [$\beta = 1.0$ (Table 1)] and A_2' contains two actin subunits. We did not, however, detect any increase in elongation rate at concentrations of actobindin as low as 300 nM (Table 3). One trivial explanation for this discrepancy could be that β may be significantly smaller than 1.0; the 95% confidence interval was 0.5−2.2 (Table 1). The ratio, β, is relatively poorly determined because relatively large changes in β have only a small effect on $d[A_2']/dt$, eq 6, and even less effect on $d[A_f]/dt$, eq 8. Nonetheless, β was estimated sufficiently accurately to predict the results of the elongation assay (Table 3). In this regard, it is important to note that the theoretical values in Table 3 were calculated using equilibrium constants (Table 1) derived from the experiment shown in Figure 1 rather than choosing equilibrium constants that best fit the data in Figure 2, and therefore, the accuracy of these theoretical values reflects the predictive power of the equilibrium constants.

Alternatively, a more complicated model in which A_2B, in addition to A_2', can add to elongating filaments might be compatible with the data. If this were the case, actobindin would have to dissociate from the end of the filament to allow further elongation, and high concentrations of actobindin would prevent this uncapping and block elongation, giving rise to the results reported in Figure 2. Possibly other, more complicated, models could be found that would fit the data, but importantly, the stoichiometric model does not.

Previously, we found (Bubb et al., 1991) that, under nonpolymerizing conditions, actobindin could simultaneously bind two actin subunits but very likely with negative cooperativity and an α of 0.6−0.9 (an α greater than 1 indicates positive cooperativity and an α less than 1 indicates possible negative cooperativity). In polymerizing conditions, we now find positive cooperativity for the interaction of two actin subunits with actobindin and an α of 59 (Table 1). This is the first thermodynamic evidence that actobindin simultaneously makes use of both actin binding sites to bind to a non-cross-linked actin oligomer.

Of greater interest is the confirmation of our earlier proposal (Bubb et al., 1994b) that actobindin causes the

formation of actin dimers that can participate in filament elongation but do not nucleate or self-associate. By inhibiting spontaneous nucleation while allowing elongation, actobindin *in situ* could prevent formation of a random network of actin filaments (for example, at the leading edge of a motile cell) without affecting the orderly elongation of uncapped filaments. Indeed, since the elongation rate constant for the actobindin-generated dimer may be the same as the elongation rate constant for actin monomer, actobindin might actually accelerate the rate of elongation at the ends of uncapped filaments even while blocking formation of new filaments.

REFERENCES

Bubb, M. R., & Korn, E. D. (1991) *Methods Enzymol. 196*, 119−125.

Bubb, M. R., Lewis, M. S., & Korn, E. D. (1991) *J. Biol. Chem. 266*, 3820−3826.

Bubb, M. R., Lewis, M. S., & Korn, E. D. (1994a) *J. Biol. Chem. 269*, 25587−25591.

Bubb, M. R., Knutson, J. R., Porter, D. K., & Korn, E. D. (1994b) *J. Biol. Chem. 269*, 25592−25597.

Estes, J. E., Selden, L. A., & Gershman, L. C. (1981) *Biochemistry 20*, 708−712.

Knott, G. D. (1979) *Comput. Programs Biomed. 10*, 271−280.

Kouyama, T., & Mihashi, K. (1981) *Eur. J. Biochem. 114*, 33−38.

Lambooy, P. K., & Korn, E. D. (1986) *J. Biol. Chem. 261*, 10785−10792.

Lambooy, P. K., & Korn, E. D. (1988) *J. Biol. Chem. 263*, 12836−12843.

Spudich, J. A., & Watt, S. (1971) *J. Biol. Chem. 246*, 4865−4871.

Tobacman, L. S., & Korn, E. D. (1983) *J. Biol. Chem. 258*, 3207−3214.

Tobacman, L. S., Brenner, S. L., & Korn, E. D. (1983) *J. Biol. Chem. 258*, 8806−8812.

Vancompernolle, K., Vandekerckhove, J., Bubb, M. R., & Korn, E. D. (1991) *J. Biol. Chem. 266*, 15427−15431.

Vandekerckhove, J., Van Damme, J., Vancompernolle, K., Bubb, M. R., Lambooy, P. K., & Korn, E. D. (1990) *J. Biol. Chem. 265*, 12801−12803.

BI942651B